Distinct Uptake mechanisms but similar intracellular processing of two different toll-like receptor ligand-peptide conjugates in dendritic cells

Khan, S.; Bijker, M.S.; Weterings, J.J.; Tanke, H.J.; Adema, G.J.; Hall, T. van; ... ; Ossendorp, F.

THE JOURNAL OF BIOLOGICAL CHEMISTRY VOL. 282, NO. 29, pp. 21145–21159, July 20, 2007

Distinct Uptake Mechanisms but Similar Intracellular Processing of Two Different Toll-like Receptor Ligand-Peptide Conjugates in Dendritic Cells*

Received for publication, February 27, 2007, and in revised form, April 13, 2007 Published, JBC Papers in Press, April 26, 2007, DOI 10.1074/jbc.M701705200

Selina Khan[‡], Martijn S. Bijker[‡1], Jimmy J. Weterings[§1], Hans J. Tanke[¶], Gosse J. Adema[‖], Thorbald van Hall[**], Jan W. Drijfhout[‡], Cornelis J. M. Melief[‡], Hermen S. Overkleeft[§], Gijsbert A. van der Marel[§], Dmitri V. Filippov[§], Sjoerd H. van der Burg[**], and Ferry Ossendorp[‡2]

*From the [‡]Departments of Immunohematology and Blood Transfusion, [¶]Molecular Cell Biology, and **Clinical Oncology, Leiden University Medical Centre, P. O. Box 9600, 2300 RC Leiden, The Netherlands, [§]Leiden Institute of Chemistry, Leiden University, P. O. Box 9502, 2300 RA Leiden, The Netherlands, and [‖]Immunology Laboratory, Radboud University Nijmegen Medical Centre, 6500 HB Nijmegen, The Netherlands*

Covalent conjugation of Toll-like receptor ligands (TLR-L) to synthetic antigenic peptides strongly improves antigen presentation *in vitro* and T lymphocyte priming *in vivo*. These molecularly well defined TLR-L-peptide conjugates, constitute an attractive vaccination modality, sharing the peptide antigen and a defined adjuvant in one single molecule. We have analyzed the intracellular trafficking and processing of two TLR-L conjugates in dendritic cells (DCs). Long synthetic peptides containing an ovalbumin cytotoxic T-cell epitope were chemically conjugated to two different TLR-Ls the TLR2 ligand, Pam_3CysSK_4 (Pam) or the TLR9 ligand CpG. Rapid and enhanced uptake of both types of TLR-L-conjugated peptide occurred in DCs. Moreover, TLR-L conjugation greatly enhanced antigen presentation, a process that was dependent on endosomal acidification, proteasomal cleavage, and TAP translocation. The uptake of the CpG~ conjugate was independent of endosomally-expressed TLR9 as reported previously. Unexpectedly, we found that Pam~conjugated peptides were likewise internalized independently of the expression of cell surface-expressed TLR2. Further characterization of the uptake mechanisms revealed that TLR2-L employed a different uptake route than TLR9-L. Inhibition of clathrin- or caveolin-dependent endocytosis greatly reduced uptake and antigen presentation of the Pam-conjugate. In contrast, internalization and antigen presentation of CpG~conjugates was independent of clathrin-coated pits but partly dependent on caveolae formation. Importantly, in contrast to the TLR-independent uptake of the conjugates, TLR expression and downstream TLR signaling was required for dendritic cell maturation and for priming of naïve $CD8^+$ T-cells. Together, our data show that targeting to two distinct TLRs requires distinct uptake mechanism but follows similar trafficking and intracellular processing pathways leading to optimal antigen presentation and T-cell priming.

Toll-like receptors (TLR)[3] are germ line-encoded receptors expressed mainly on cells of the innate immune system, such as granulocytes, macrophages, and dendritic cells (DCs). These receptors are important in sensing infectious agents through recognition of pathogen-associated molecules and act as a communicator between innate and adaptive immune responses. The receptors are expressed either on the cell surface or in the endosomal organelles. This compartmentalization of the TLR correlates with the type of ligands with which they interact. The TLRs expressed on the cell surface bind to extracellular components of the microorganisms (such as bacterial LPS to TLR4, bacterial lipopeptide to TLR2). In contrast, the TLRs found in the endosomes bind to ligands derived from intracellular molecules of the pathogen, such as unmethylated CpG DNA sequences to TLR9 and single-stranded RNA to TLR7 (1). Studies have shown that ligands interacting with the latter type of TLRs are internalized independently of the TLRs (2). Upon engagement of the ligand to its receptor, a cascade of intracellular signaling events is initiated that involves docking of different adaptor molecules such as MyD88 and TRAM to the TLR receptors and recruitment of proteins belonging to the IRAK-family, which ultimately culminate in the activation of the NF$\kappa\beta$ transcription factor and gene transcription leading to production of proinflammatory cytokines (3).

DCs are both initiators and regulators of T cell responses (4). Dendritic cells constantly screen the environment for potential foreign antigens by a variety of mechanisms such as phagocytosis, macropinocytosis, caveolin-mediated, or clathrin-dependent endocytosis. The manner of uptake is dependent on the size and nature of material to be internalized (5, 6). As specialized antigen-presenting cells, DCs have the capacity to

* This work has been funded by Netherlands Organization for Scientific Research as a part of the From Molecule to Cell program (to S. H. v B., D. V. F., G. A. M., and F. O.) and by the KWF Kankerbestrijding UL 2003-2817 (to S. H. v B.). The costs of publication of this article were defrayed in part by the payment of page charges. This article must therefore be hereby marked "*advertisement*" in accordance with 18 U.S.C. Section 1734 solely to indicate this fact.

[1] These authors contributed equally.

[2] To whom correspondence should be addressed. Tel.: 31-71-5263843; Fax: 31-71-5265267; E-mail: f.a.ossendorp@lumc.nl.

[3] The abbreviations used are: TLR, Toll-like receptor; TLR-L, TLR ligand; DC, dendritic cell; BMDC, bone marrow-derived DC; CTL, cytotoxic T-cell lymphocyte; MDC, monodansylcadaverine; MFI, mean fluorescence intensity; MHC, major histocompatibility complex; ODN, oligonucleotide; Pam, Pam_3CysSK_4; s.c., subcutaneous; TM, tetramer; MALDI, matrix-assisted laser desorption ionization; LPS, lipopolysaccharide; Fmoc, *N*-(9-fluorenyl)methoxycarbonyl; HPLC, high performance liquid chromatography; ACN, actonitrile; IL, interleukin; WT, wild type; TAP, transporter associated with antigen processing; HCTU, 1-[bis(dimethylamino)methylene]-5-chloro-1H-benzotriazolium 3-oxide hexafluorophosphate; DMT, 4,4′-dimethoxytrityl; NMP, *N*-methylpyrrolidone; FACS, fluorescence-activated cell sorter; TAC, *tert*-butylphenoxyacetyl.

efficiently process exogenous proteins and present the peptides in major histocompatibility complex (MHC) class I molecules, a process known as cross-presentation. In this scenario exogenously derived antigens are internalized and translocate from the endosomal route into the cytosol, where the proteasome complex processes the antigen. The generated peptides are transported from the cytosol into the endoplasmic reticulum via the peptide transporter TAP (7), after which the peptides undergo further trimming and are finally loaded onto MHC class I molecules, which translocate to the cell surface, where the peptide is presented to $CD8^+$ T-cells.

The ability of DCs to cross-present peptides on MHC class I to $CD8^+$ T-cells together with the capacity of TLR ligands to deliver maturation signals has inspired efforts to explore the use of DCs as a vaccine vehicle in the fight against infectious diseases and cancer (8, 9). Covalent linkage of immunogenic peptides to the TLR9 ligand, CpG DNA, or TLR2 ligands, like Pam_3CysSS and Pam_3CysSK_4, induces a more prominent T-cell response than administration of free TLR2-L or TLR9-L mixed with protein (2, 10–16).

To explore the mode of action of TLR-L antigen conjugates, we have designed well defined synthetic vaccines composed of peptides containing the model antigen ovalbumin $CD8^+$ cytotoxic T-lymphocyte (CTL) epitope (SIINFEKL) chemically linked to either the TLR2-ligand, Pam_3CysSK_4, or the TLR9 ligand, CpG. These conjugates were used to study the uptake, intracellular routing, and processing. We show that not only TLR9-L conjugates but also the TLR2-L conjugates are taken up independently of TLR expression albeit through two distinct internalization mechanisms. Down-stream processing route for MHC class I antigen presentation, however, were similar and requires endosomal acidification, TAP translocation, and proteasomal processing. Importantly, whereas the uptake of both types of TLR-L conjugates was independent of TLR expression, priming of specific $CD8^+$ T-cell response required TLR signaling in dendritic cells.

EXPERIMENTAL PROCEDURES

Mouse Strains and Chemicals

C57BL/6 (B6; H-2^b) were obtained from Charles River Laboratories. TLR2-deficient mice were purchased from Jackson Laboratories, whereas the TLR9-deficient mice were obtained from S. Akira Osaka University, Osaka, Japan. Bone marrow from TAP-deficient mice and TAP/β2-microglobulin-deficient mice strains was kindly provided by Prof. H. G. Ljunggren, Karolinska Institutet, Sweden. LPS of *Escherichia coli* (serotype026:B6), Monodansylcadaverine (MDC), and filipin were purchased from Sigma-Aldrich. Epoxomicin and chlorophenol red-β-D-galactopyranoside were from Calbiochem.

Cell Lines

Freshly isolated DCs were cultured from mouse bone marrow cells as described elsewhere (17). D1 cell line, a long term growth factor-dependent immature splenic DC line derived from B6 (H-2^b) mice, was cultured as described (18). B3Z is a T-cell hybridoma specific for the H-$2K^b$ CTL epitope SIINFEKL that expresses a β-galactosidase construct under the regulation of the NF-AT element from the IL2 promoter (19). EG7 (EL4-OVA) (20) was cultured in complete medium with 400 μg of G418 (Invitrogen).

Generation of Pam_3CysSK_4- or CpG-conjugated Peptides and Labeling

Table 1 shows the conjugates and peptides used in this study.

Chemicals

HCTU was purchased from IRIS Biotech GmbH (Germany), and Pam_3Cys-OH was from Bachem. PyBOP (benzotriazole-1-yl-oxytrispyrrolidinophosphonium hexafluorophosphate) was purchased from MultiSynTech GmbH. Reactive fluorescent dyes BODIPY-FL *N*-(2-aminoethyl) maleimide, Alexa Fluor 488 C_5 maleimide, and Alexa Fluor 488 carboxylic acid succinimidyl ester were purchased from Invitrogen. Fmoc amino acids were from SENN Chemicals or from MultiSynTech GmbH. Tentagel-based resins were purchased at Rapp Polymere GmbH. All chemicals and solvents used in the solid phase peptide synthesis were from Biosolve. Chemicals, resins, and solvents used in the solid phase DNA synthesis except Beaucage reagent and Control Pore Glass support used to introduce 3′-thiol modification were from Proligo and were used as received. 3′-Thiol modifier C3 S-S Control Pore Glass and Beaucage reagent were purchased at Glen Research. All chemicals were used as received.

General Methods

Mass spectra were recorded on a PE SCIEX API 165 (PerkinElmer Life Sciences) mass spectrometer. Analytical liquid chromatography/mass spectroscopy was conducted on a Jasco system using an Alltima C_{18} analytical column (4.6 × 150 mm, 5-μm particle size, flow 1.0 ml/min) with detection at 214 and 254 nm. The solvent system was 100% water (A), 100% acetonitrile (B), and 1% trifluoroacetic acid (C). Gradients of A to B were applied over 15 min, keeping C isocratic at 10%. Purifications of the synthetic peptides were conducted on a BioCAD Vision automated HPLC system (PerSeptive Biosystems, Inc.) supplied with a Alltima C_{18} column (10 × 250 mm, 5-μm particle size, running at 4 ml/min). A Varian DMS 200 UV-visible spectrophotometer was used to measure UV absorption MALDI-time-of-flight spectra were recorded on a Voyager-DE PRO mass spectrometer (Perseptive Biosystems, Inc.).

Peptide Synthesis

Fmoc-based solid-phase peptide synthesis was performed on a CS Bio 336 automated instrument (CS Bio Co.) starting from either preloaded Fmoc-Leu-PHB-Tentagel resin or from Tentagel -RAM resin. The synthesis was performed on a 50- or 250-μmol scale according to established methods (21). HCTU was used as coupling reagent. All peptides (see Table 1) were cleaved from the resin using trifluoroacetic acid/triisopropylsilane/H_2O (95/2.5/2.5) for 2 h at room temperature, precipitated from diethyl ether, redissolved in 20% aqueous 1,1,1,3,3,3-hexafluoro-2-propanol, and purified by reverse phase HPLC and characterized using liquid chromatography/mass spectroscopy and MALDI mass spectroscopy (see "General Methods").

Oligonucleotide Synthesis

DMT-based solid-phase phosphorothioate oligonucleotide (ODN) synthesis was performed on an Expedite automated instrument (Perseptive Biosystems) starting from Control Pore Glass support with the 3′-thiol modifier. The syntheses were performed on a 10-μmol scale according to established methods (22). Elongation was performed using 3′-phosphoramidite derivatives of DMT-protected nucleosides 5′-DMT-A(TAC)-OH, 5′-DMT-C(TAC)-OH, 5′-DMT-G(TAC)-OH, and 5′-DMT-T-OH under the agency of dicyanoimidazole. After each coupling, remaining free 5′-hydroxyls were blocked using a capping solution (*t*-butylphenoxyacetic anhydride (Tac_2O)/1-methylimidazole in tetrahydrofuran/pyridine) followed by sulfurization of the phosphite linkage to the phosphorothioate linkage using the Beaucage reagent. Next, the 5′-DMT protecting group was removed by trichloroacetic acid, after which elongation was continued. After final DMT removal the DNA oligomer was cleaved from the resin by 25% ammonium hydroxide solution to give a 3′-disulfide modified ODN (ODN-SS-propyl-OH). ODNs were purified on a Q-Sepharose column pre-equilibrated with 50 mM NaOAc applying a gradient of 2 M NaCl in 50 mM NaOAc. Fractions containing the pure product were combined and dialyzed three times with Millipore water using dialysis tubing with 1-kDa cut-off (Spectrum). Quantification was performed by UV absorbance at 260 nm. Sequences of the ODN prepared in this study were CpG, 5′-TCCATGACGTTCCTGACGTT-3′; GpC, 5′-TCCATGAGCTTCCTGATG-3′.

Maleimidopropionoyl Peptides Mal-$OVA_{247–264}$ and Mal-$OVA_{247–264A5K}$

Fmoc-deprotected peptide resin (200 mg, 30 μmol) was suspended in 2 ml of NMP, and 3-maleimidopropionic acid (5 eq, 250 μmol, 42.2 mg), HCTU (5 eq, 250 μmol, 103.2 mg), and *N*,*N*′-diisopropylethylamine (5 eq, 250 μmol, 42 μl) were added subsequently. The mixture was shaken for 2 h after which the resin was filtered, washed with NMP, dichloromethane, and dried. A 2,4,6-trinitrobenzenesulfonic acid test indicated complete coupling. The products were processed as described under "Peptide Synthesis."

ODN-Peptide Conjugates

For CpG-$OVA_{247–264}$, 3′-disulfide modified CpG-SS-propyl-OH (266 nmol) was converted to 3′-SH-modified CpG-SH overnight with dithiothreitol (DTT)-containing buffer (35 mg of DTT, 26 mg of NaOAc·$3H_2O$, 1 ml of water). Dithiothreitol was removed from the mixture using a PD-10 desalting column (Amersham Biosciences) that was pre-equilibrated with 25 ml of a 50 mM phosphate buffer (25 mM Na_2HPO_4, 25 mM NaH_2PO_4, 1 mM EDTA in water, continuously degassed with helium. Filtrate (3.25 ml) was directly transferred to a tube containing 5 mg of maleimidopropionyl peptide Mal-$OVA_{247–264}$. The resulting solution was sonicated and placed under blanket of argon. The tube was sealed and shaken for 2 days at room temperature. The mixture was purified over a Superdex 75 gel filtration column using isocratic elution with 0.15 M triethylammonium acetate. Fractions containing the product were collected and lyophilized. Excess triethylammonium acetate was removed by lyophilization from water (3 times). Quantification was performed by UV absorbance (260 nm). CpG-$OVA_{247–264A5K}$ and GpC-$OVA_{247–264}$ were prepared as described for CpG-$OVA_{247–264}$ starting from the corresponding ODNs and maleimidopropionyl peptides.

Lipopeptides

For Pam_3CysSK_4-$OVA_{247–264}$, Fmoc-deprotected peptide resin (300 mg, 45 μmol) was suspended in 1.4 ml or 1:1 NMP/dichloromethane. Pam_3Cys-OH (91 mg, 2 eq, 100 μmol) and PyBOP (benzotriazole-1-yl-oxytrispyrrolidinophosphonium hexafluorophosphate; 80 mg, 3 eq, 150 μmol) were added. *N*,*N*′-Diisopropylethylamine (30 μl, 175 μmol) was added in two portions of 15 μl with an interval of 15 min, and the mixture was shaken for 4 h.[4] The resin was washed with NMP and dichloromethane and dried. A 2,4,6-trinitrobenzenesulfonic acid test indicated complete coupling. The product was cleaved from the resin as described under "Peptide Synthesis," dissolved in *t*-butyl alcohol/ACN/H_2O (1:1:1), and purified on an Alltima CN column (10 × 250 mm, 5-μm particle size) with a gradient of A to B; C was kept isocratic at 10% (A, 1:1 CH_3OH/H_2O; B, ACN; C, 1% trifluoroacetic acid in 9:1 CH_3OH/H_2O). Pam_3CysSK_4-$OVA_{247–264A5K}$ and Pam_3CysSK_4C-$OVA_{247–264}$ were prepared and purified as described above for Pam_3CysSK_4-$OVA_{247–264}$ starting from the corresponding peptide resins.

Fluorescently Labeled Peptides and Conjugates

[Alexa488]$OVA_{247–264}$—Fmoc-deprotected peptide resin (100 mg, 15 μmol) was treated twice with 2 ml of a capping reagent (0.5 M Ac_2O, 0.125 M *N*,*N*′-diisopropylethylamine in NMP). A 2,4,6-trinitrobenzenesulfonic acid test indicated complete acetylation. The cleaved and purified peptide (1 mg) was dissolved into 50 μl of buffer (300 mM $NaHCO_3$ in 30% acetonitrile/water), and Alexa Fluor 488 carboxylic acid succinimidyl ester (0.3 mg) was added. Another 50 μl of buffer was added, and the mixture was shaken overnight. The product was purified by reverse phase HPLC (see "General Methods").

CpG-[Alexa488]$OVA_{247–264}$ *and GpC-[Alexa488]*$OVA_{247–264}$—Conjugate CpG-$OVA_{247–264}$ (296 nmol) or GpC-[Alexa488]$OVA_{247–264}$ (296 nmol) was dissolved in 50 μl of buffer (300 mM $NaHCO_3$, 30% ACN in H_2O), and Alexa Fluor 488 carboxylic acid succidinimidyl ester (1.0 mg) was added. The bright green mixture was shaken overnight. The mixture was diluted 5 times with H_2O before being subjected to reverse phase HPLC purification. (Alltima C_{18}, gradient of A to B; C was kept isocratic at 10%; A, H_2O; B, ACN; C, 100 mM aqueous NH_4OAc).

Pam_3CysSK_4-C[BDP-FL]$OVA_{247–264}$—Lipopeptide Pam_3CysSK_4C-$OVA_{247–264}$ (0.46 μmol, 1.69 mg) and BODIPY-FL *N*-(2-aminoethyl)maleimide were transferred to a vial containing 0.5 ml of 50 mM phosphate buffer (25 mM NaH_2PO_4, 25 mM Na_2HPO_4, 1 mM EDTA in 2:1:1 H_2O/ CH_3OH /ACN). The mixture was sonicated and shaken for 60 h under argon. The

[4] The use of a large excess of *N*,*N*′-diisopropylethylamine (4 eq relative to Pam_3Cys-OH) proved to be detrimental for the purity of the product as judged by liquid chromatography/mass spectroscopy analysis.

mixture was diluted 5 times with 40:30:30 H_2O/ACN/*t*-butyl alcohol, 1% trifluoroacetic acid before being subjected to reverse phase HPLC purification as described for $Pam_3CysSK_4C\text{-}OVA_{247-264}$.

SK_4-C[BDP-FL]-$OVA_{247-264}$—SK_4-C[BDP-FL]-$OVA_{247-264}$ was synthesized as described for Pam_3CysSK_4-C[BDP-FL]$OVA_{247-264}$ using 50 mM phosphate in 3:2 H_2O/ACN as a ligation buffer and SK_4-C-$OVA_{247-264}$ as the peptide substrate. Pam_3CysSK_4-C[Alexa488]$OVA_{247-264}$ was synthesized as described for Pam_3CysSK_4-C[BDP-FL]$OVA_{247-264}$ using Alexa Fluor 488 C_5 maleimide as the reactive dye.

IL-12p40 Enzyme-linked Immunosorbent Assay—DCs (4×10^4) were plated into a 96-well round bottom plate and incubated for 24–48 h with the compounds indicated in the legend to Fig. 1. Supernatants were harvested and tested for IL-12 p40/p70 content using a standard sandwich enzyme-linked immunosorbent assay as previous described (23).

Confocal Microscopy

DCs were plated out into glass-bottom Petri dishes (MatTek) 2 days before the experiment. Cells were incubated either with the fluorescence-labeled TLR-L peptide conjugate or the fluorescence-labeled peptide at 37 °C for different time periods at the concentrations indicated in the figure legends. In some experiments, as indicated, cells were coincubated with 1 μM Lysotracker for 5 min to stain endosomal/lysosomal compartments. In experiments with inhibitors, cells were preincubated for 30 min either with 50 μM MDC or 10 μg/ml filipin followed by extensively washing before incubation with the TLR-L conjugate either alone (pretreatment) or in the presence of inhibitors (coincubation). Cells were then washed and imaged using an inverted Leica SP2 confocal microscope. Dual color images were acquired by sequential scanning, with only one laser line per scan to avoid cross-excitation. The images were processed using the software program ImageJ.

Flow Cytometry

For analyzing the effect of the different compounds on dendritic cell phenotypic profile, DCs were incubated with the different compounds at a final concentration of 1 μM for 48 h. Subsequently, cells were harvested, resuspended in fluorescence-activated cell buffer (phosphate-buffered saline, 0.1% bovine serum albumin), and incubated for 20 min with the following panel of monoclonal antibodies: fluorescein isothiocyanate-anti-CD86 (clone GL-1), phycoerythrin-anti-I-A^b (clone M5/114 15.2), phycoerythrin- anti-CD40 (clone 3/23), allophycocyanin-anti-K^b (24). Cells were washed twice and fixed with 0.5% paraformaldehyde before being subjected to flow cytometry measurements.

MHC Class I-restricted Antigen Presentation Assay

DCs were incubated for 2 h (unless stated otherwise in the legends to Figs. 6 and 8) with 1) the parent peptide (DEVSGLEQLESIINFEKLAAAAAK, $OVA_{247-264A5K}$, or DEVSGLEQLESIINFEKL, $OVA_{247-264}$), 2) the peptide conjugate, or 3) the mixture of the parent peptide and the Pam_3CysSK_4 or CpG at the indicated concentrations. Cells were washed five times with medium before the T-cell hybridoma B3Z cells were added and incubated for 16h at 37 °C.

Antigen presentation of the ovalbumin cytotoxic T-cell epitope SIINFEKL ($OVA_{257-264}$) in H-$2K^b$ was detected by activation of B3Z cells measured by a colorimetric assay using chlorophenol red-β-D-galactopyranoside as substrate to detect *lacZ* activity in B3Z lysates, as described (23).

In some experiments cells were preincubated for 30 min with titrated amounts of epoxomicin ranging from 0.01 to 10 μM epoxomicin or with 3 mM NH_4Cl or preincubated for 60 min with titrated amounts of monodansylcadaverine (25–50 μM) or with filipin (10–20 μg/ml) before adding the peptide compound still in the presence of the inhibitors. Cell viability was confirmed by tryphan blue exclusion at the indicated concentration range of inhibitors.

Priming of Endogenous Naïve $CD8^+$ T-cells

To determine the endogenous CTL response, five nmol of the different compounds were injected s.c. into naïve C57BL/6 mice. After 10 days spleen cells were stimulated *in vitro* by plating 10×10^6 splenocytes with 1×10^6 mytomycin C (Kyowa)-treated (50 μg/ml for 1 h at 37 °C) and -irradiated (4000 rads) EG7 cell line (EL4-OVA) in the absence of additional cytokines. After 7 days viable splenocytes were isolated over a Ficoll gradient and stained for H-$2K^b$ tetramer (TM)-$OVA_{257-264}$, CD8b2 (clone 53-5.8) and propidium iodide to exclude dead cells as described previous (23).

Intracellular Cytokine Staining

An aliquot of spleen cells after re-stimulation and Ficoll purification (see above) were subjected to stimulation *in vitro* with or without 1 μg/ml $OVA_{257-264}$ peptide (H2-K^b restricted SIINFEKL) overnight in the presence of GolgiPlug (BD Pharmingen). Cells were then washed twice with fluorescence-activated cell sorter buffer and stained with phycoerythrin-conjugated monoclonal rat anti-mouse CD8b2 antibody. Cells were subjected to intracellular cytokine staining using the Cytofix/Cytoperm kit according to the manufacturer's instructions (BD Pharmingen). Intracellular interferon-γ was stained with allophycocyanin-conjugated rat anti-mouse interferon-γ. All antibodies were purchased from BD Pharmingen. Flow cytometry analysis was performed using FACSCalibur with CELLQuest software (BD Biosciences). Splenocytes without peptide stimulation were used as a negative control.

In Vivo Uptake Studies

To monitor the uptake of the TLR-L-conjugated peptides and the free peptide *in vivo*, mice were injected s.c. either with 5 nmol of Alexa488 Fluor-labeled CpG~conjugated peptide, 5 nmol of BODIPY-FL Pam~conjugated peptide, CpG mixed with Alexa488 Fluor-labeled peptide, or Pam mixed with BODIPY-FL-labeled peptide. Three days later mice were sacrificed, and a single cell suspension of the draining lymph nodes was stained for CD11c (clone HL3) before being subjected to flow cytometry analysis.

RESULTS

To study the uptake, trafficking, and processing of two distinct TLR-ligand peptide conjugates in dendritic cells for MHC

TABLE 1

List of compounds generated

The bold and underlined residues were used to couple the indicated fluorophores.

Abbreviation	TLR ligand	Peptide	Fluorophore
$OVA_{257-264}$		SIINFEKL	
$OVA_{247-264}$		DEVSGLEQLESIINFEKL	
$OVA_{247-264A5K}$		DEVSGLEQLESIINFEKLAAAAAK	
CpG-$OVA_{247-264}$	CpG	DEVSGLEQLESIINFEKL	
CpG-$OVA_{247-264A5K}$	CpG	DEVSGLEQLESIINFEKLAAAAAK	
GpC-$OVA_{247-264}$	GpC	DEVSGLEQLESIINFEKL	
Pam_3CysSK_4-$OVA_{247-264}$	Pam_3CysSK_4	DEVSGLEQLESIINFEKL	
Pam_3CysSK_4-$OVA_{247-264A5K}$	Pam_3CysSK_4	DEVSGLEQLESIINFEKLAAAAAK	
[Alexa488]$OVA_{247-264}$		Ac-DEVSGLEQLESIINFE**K**L	Alexa488
SK_4-C[BDP-FL]-$OVA_{247-264}$		SKKKK**C**DEVGLEQLESIINFEKL	Bodipy-FL
CpG-[Alexa488]$OVA_{247-264}$	CpG	DEVSGLEQLESIINFE**K**L	Alexa488
GpC-[Alexa488]$OVA_{247-264}$	GpC	DEVSGLEQLESIINFE**K**L	Alexa488
Pam_3CysSK_4-C[Alexa488]$OVA_{247-264}$	Pam_3CysSK_4	**C**DEVSGLEQLESIINFEKL	Alexa488
Pam_3CysSK_4-C[BDP-FL]$OVA_{247-264}$	Pam_3CysSK_4	**C**DEVSGLEQLESIINFEKL	Bodipy-FL

class I presentation to $CD8^+$ cytotoxic T-lymphocytes, we selected the TLR9 ligand CpG and the TLR2 ligand Pam_3CysSK_4 (Pam) based on the fact that these two ligands interact with two distinct receptors located either in the endosomal compartment (TLR9) or on the plasma membrane (TLR2). As a model antigen we made use of peptides containing the CTL epitope (SIINFEKL, designated $OVA_{257-264}$) derived from the ovalbumin protein. Two different peptide length variants were synthesized, an extended peptide that required proteasome-dependent processing on both the N and C terminus to release the CTL epitope (DEVSGLEQLESIINFEKLAAAAAK) designated $OVA_{247-264A5K}$, and a shorter peptide, of which C-terminal processing by the proteasome is not required (DEVSGLEQLESIINFEKL), designated $OVA_{247-264}$. For example, peptide $OVA_{247-264A5K}$ conjugated to Pam_3CysSK_4 is designated as Pam~$OVA_{247-264A5K}$.

Crucially, all of our compounds (listed in Table 1) are produced synthetically and are, therefore, chemically well defined, of high purity, and of constant quality, avoiding potential contamination with other TLR ligands such as LPS, which commonly occur in purified TLR ligand preparations.

Robust Induction of Naïve CD8-specific T-cells Mediated by the Conjugates—To establish the quality of our generated TLR-L-peptide conjugates, we first investigated the induction of an endogenous T-cell response following s.c. injection of either TLR-L-conjugated peptide or free peptide into naïve C57BL/6 mice. After 10 days, the induction of $OVA_{247-264}$-specific $CD8^+$ T-cells was analyzed. As is shown in Fig. 1*A*, the magnitude of the $OVA_{257-264}$-specific T-cell response induction by either CpG~$OVA_{247-264A5K}$ or Pam~$OVA_{247-264A5K}$ was significantly higher than that in mice injected with non-conjugated $OVA_{247-264A5K}$ peptide mixed together with either free CpG or free Pam. To address whether the induction of specific T-cells depended on activation of the DCs, we injected GpC~$OVA_{247-264}$ conjugate, which is a non-stimulatory oligonucleotide, as shown by its lack of capacity to induce IL-12 production by DCs (Fig. 1*C*). Injection of the GpC~peptide conjugate into naïve mice led to a significantly lower induction of specific $CD8^+$ T-cells than of CpG~conjugated peptide but was still as high as the response obtained after mixing of peptide with the CpG (Fig. 1*A*). Importantly, only when a stimulatory TLR-L conjugate was given, were the majority of $CD8^+$ T-cells able to produce interferon-γ (Fig. 1*B*), indicating that signaling via the TLR is essential for the generation of large numbers of functional T-cells *in vivo*. These results suggest that the enhanced induction of specific T-cells is primarily the result of efficient delivery of the TLR-L-conjugated peptide into the antigen-presenting cell.

TLR Conjugates Activate Dendritic Cells—Next we analyzed the ability of the different conjugates to induce maturation of DCs. As evident from Table 2, increased surface marker expression of CD40, CD86, MHC I, and MHC II was observed in dendritic cells after treatment with the different TLR-L conjugates to a similar extent as the free TLR-Ls. To confirm the involvement of the TLRs in DC activation, we isolated bone marrow-derived dendritic cells (BMDCs) from wild type (WT) mice, TLR2-deficient mice, and TLR9-deficient mice and stimulated these cells with the different conjugates followed by phenotypic characterization by staining for different surface markers associated with DC maturation (25). No up-regulation of the cell surface markers CD86 and MHC class II was detected when BMDCs from TLR2-deficient mice or TLR9-deficient mice were stimulated with Pam~conjugated peptide or CpG~conjugated peptide, respectively (Fig. 2). This impaired up-regulation was not due to a general defect in the maturation signaling pathway, because stimulation with LPS could induce up-regulation of CD86 and MHC II in BMDCs derived from both TLR2- and TLR9-deficient mice to a similar extent as observed for BMDCs derived from wild type mice. Taken together, these results demonstrate that the conjugates are as effective as free TLR ligand in activating the DCs and show that the expression of the cognate TLR is required for activation of DCs by the TLR-L-peptide conjugates.

Efficient Uptake of CpG- and Pam-conjugated Antigen Peptides by Dendritic Cells—Having demonstrated that TLR signaling was important for DC activation and priming of T-cells, we decided to compare the downstream cellular mechanism used by the two types of TLR-L with respect to uptake, routing, and cellular processing. Therefore, the efficiency of antigen uptake of conjugated *versus* non-conjugated peptide by DCs was determined. DCs were incubated with either Pam~conjugated peptide or free peptide. Both compounds were labeled with a fluorophore (attached on the peptide backbone), which allowed us to monitor the internalization of these compounds by confocal microscopy analysis. Introduction of the fluorophore (either

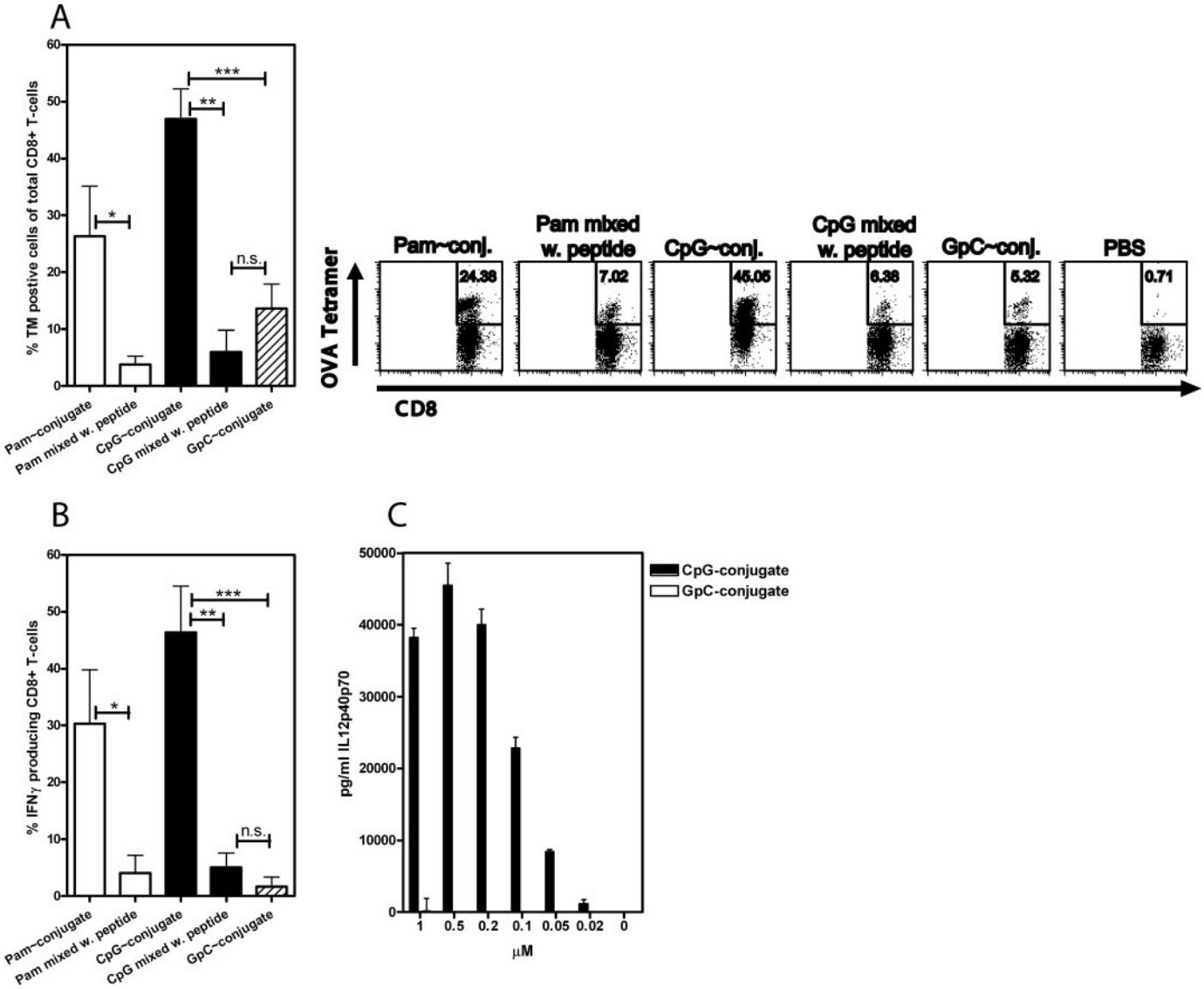

FIGURE 1. **Robust induction of naïve CD8$^+$-specific T-cells mediated by the TLR-L conjugates.** *A*, naïve C57/B6 mice were injected with either Pam mixed with $OVA_{247–264A5K}$ (*Pam mixed w. peptide*), Pam~$OVA_{247–264A5K}$ (*Pam~conjugate*), CpG mixed with $OVA_{247–264A5K}$ (*CpG mixed w. peptide*), CpG~$OVA_{247–264A5K}$ (*CpG~ conjugate*), or GpC~$OVA_{247–264}$ (*GpC~conjugate*). After stimulation *in vitro*, cells were analyzed for the presence of CD8b2 cells capable of interacting with H-2K^b-$OVA_{257–264}$ tetrameric complexes. The *y* axis displays the percentages of tetrameric-positive cells out of total CD8b2+ cells. The percent of tetrameric CD8b2+ cells (<1%) of the naïve mice (phosphate-buffered saline (*PBS*) injection only) has been subtracted from all the values. The *right-hand panel* shows a representative FACS plot; cells were gated on CD8$^+$, and the percentages given in the *top* of the *right quadrant* are the percentages of tetramer-positive cells of total CD8$^+$ T cells. Unpaired Student's *t* test error: *, $p = 0.04$; **, $p = 0.0006$; ***, $p = 0.001$; *n.s.*, not significant. *B*, interferon-γ (*IFN*) production in specific T-cells was measured as described under "Experimental Procedures." Shown are results gated on CD8$^+$ events. Pam mixed with $OVA_{247–264A5K}$ (*Pam mixed w. peptide*), Pam~$OVA_{247–264A5K}$ (*Pam~conjugate*), CpG mixed with $OVA_{247–264A5K}$ (*CpG mixed w. peptide*), CpG~$OVA_{247–264A5K}$ (*CpG~conjugate*), or GpC~$OVA_{247–264}$ (*GpC~conjugate*). Unpaired Student's *t* test error: *, $p = 0.05$; **, $p = 0.001$; ***, $p = 0.0007$; *n.s.*, not significant. Experiments were conducted with five mice per group. *C*, BMDCs were incubated either with CpG~$OVA_{247–264A5K}$ (*black bars*) or GpC~$OVA_{247–264}$ (*white bars*) for 48 h. Supernatant was harvested, and the concentration of IL-12p40 was determined as outlined under Experimental Procedures." Results are the means of triplicates ± S.E. Data are representative of three independent experiments.

Alexa488 or BODIPY-FL) into the conjugates did not alter the ability of the conjugates to activate DCs as comparable levels of the IL-12 cytokine were produced by the fluorescent conjugates and the dark conjugates.[5] As indicated by the increased intensity of fluorescence inside the cells, the Pam~conjugated peptides were taken up far more efficiently than the non-conjugated peptide (Fig. 3*A*). Interestingly, the Pam~conjugated peptide was found to accumulate in hot spots (indicated by *arrows* in Fig. 3*A*), whereas a more diffuse pattern was observed in DCs incubated with the peptide alone. Quantification of the mean fluorescence intensity (MFI) revealed a more than 4-fold higher fluorescence in DCs incubated with the Pam~conjugate compared with DCs incubated with the peptide (Fig. 3*B*). Similarly, CpG~conjugated peptide was internalized more efficiently than the unconjugated peptide by DCs (Fig. 3*C*). In addition, the non-stimulatory GpC~conjugate (MFI 63 ± 7.3) was inter-

[5] S. Khan, M. S. Bijker, J. J. Weterings, H. J. Tanke, G. J. Adema, T. van Hall, J. W. Drijfhout, C. J. M. Melief, H. S. Overkleeft, G. A. van der Marel, D. V. Filippov, S. H. van der Burg, and F. Ossendorp, unpublished data.

nalized to a similar extent as the stimulatory CpG~conjugate (MFI 72 ± 9.1) (Fig. 3*D*).

These comparisons indicate that the fluorescent TLR-L conjugates are taken up much more efficiently by DCs than unconjugated peptides *in vitro*. To examine the uptake efficiency *in vivo*, mice were injected with either Alexa488 Fluor-labeled CpG~conjugate or peptide labeled with Alexa488 Fluor mixed with dark CpG. Three days later draining lymph node cells were stained for the DC surface marker CD11c. In line with the *in vitro* results, a significantly higher proportion of $CD11c^+$ cells had taken up the CpG~conjugated peptide (2.5%) when compared with the population of DCs that ingested unconjugated peptide (0.3%) or non-injected mice (0.1%; Fig. 3*E*). A similar tendency was observed upon comparison of BOPIPY-FL-labeled Pam~conjugate with peptide labeled with BODIPY-FL mixed with dark Pam (Fig. 3*F*). Collectively, these results indicate that it is the covalent linking of the peptide to the TLR-L that is responsible for the enhanced uptake by the DCs.

TABLE 2

Cell surface marker expression after TLR-L- conjugate-induced maturation of dendritic cells

Dendritic cells were incubated for 48 h in the presence of 1 μM concentrations of either $OVA_{247–264}$ (peptide), CpG, CpG-mixed $OVA_{247–264}$ (CpG mixed with peptide), CpG ~ $OVA_{247–264}$ (CpG~conjugate), Pam, Pam mixed with $OVA_{247–264}$ (Pam mixed with peptide), Pam~$OVA_{247–264}$ (Pam~conjugate), or with *E.coli* LPS (10 μg/ml). Cells were stained with specific antibodies as described under "Experimental Procedures" and subjected to flow cytometry analysis. Indicated are the mean fluorescence intensities of positive cells. The results were obtained from a single experiment and are representative of four similar experiments. ND, not done.

Treatment	Mean fluorescence			
	CD40	CD86	MHC I	MHC II
Untreated	8	21	923	277
Peptide	8	22	ND	271
CpG	59	136	3421	512
CpG mixed with peptide	48	134	ND	903
CpG~conjugate	71	132	3229	725
Pam	16	38	ND	327
Pam mixed with peptide	18	40	ND	346
Pam~conjugate	14	35	1348	329
LPS	46	137	3572	576

Conjugates Translocate to the Endosomal/Lysosomal Compartment Independently of TLR Expression—Our antigen uptake studies revealed that also the TLR9-L conjugate was taken up more efficient despite that TLR9 is not surface-expressed. Therefore, to evaluate the relevance of TLR expression for the enhanced uptake, BMDCs purified from WT, $TLR2^{-/-}$, and $TLR9^{-/-}$ mice were incubated with Alexa488 Fluor-labeled TLR-L conjugates. As shown in Fig. 4, *A* and *C*, BMDCs from $TLR9^{-/-}$ mice internalized CpG~conjugates to a similar extent as BMDCs from wild type mice, as reported previously (2).

Surprisingly, similar experiment carried out with Pam~conjugate and BMDCs from WT mice and $TLR2^{-/-}$ mice showed that also the Pam conjugate, despite the fact that the receptor for Pam (TLR2) is located on the cell surface (1, 26), were internalized equally well by both types of DCs (Fig. 4, *B* and *D*).

To monitor the intracellular localization of the conjugates, we performed a co-localization study between the conjugates (green) and the endosomes (red). As seen in Fig. 4*E*, both the CpG~ and Pam~conjugates are co-localized partially with an endosomal tracker (Lysotracker) in a pattern characteristic for the endosomal vehicles. Moreover, no overall difference in the uptake kinetic or in the trafficking of the compounds could be detected when comparing BMDCs from wild type mice to mice deficient for either TLR9 or TLR2 expression.[5] These results indicate that TLR expression is not required for uptake and that the conjugate re-locates to the endosomal compartment.

Conjugation of Peptide Leads to Pronounced Enhancement in Antigen Presentation in Vitro—Having established that the conjugates were taken up much more efficiently than the free peptide harboring the OVA CTL epitope SIINFEKL, we next addressed the effect of conjugation of peptide to TLR-L on antigen presentation. DCs were loaded with either the CpG~conjugated peptide, Pam~conjugated peptide, the CpG

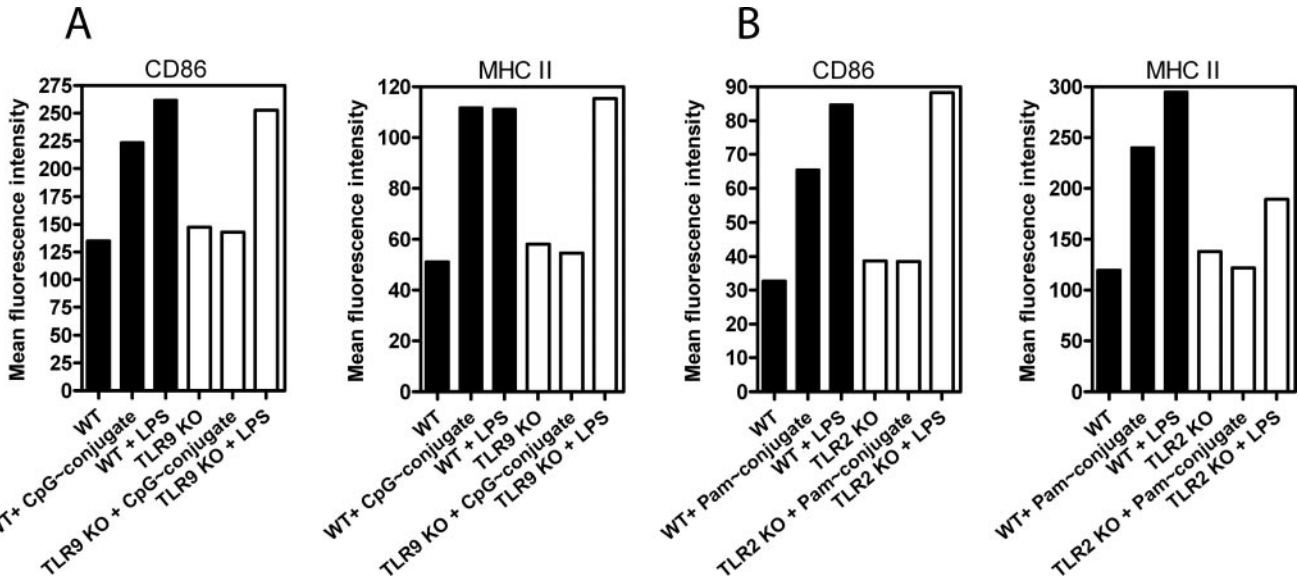

FIGURE 2. **TLR-dependent DC activation.** *A*, BMDCs from either WT or TLR9-deficient mice (*TLR9 KO*) were incubated either with 1 μM CpG~$OVA_{247–264A5K}$ or *E. coli* LPS (10 μg/ml) for 48 h. Cells were stained with CD86 or MHC II antibodies as described under "Experimental Procedures" and subjected to flow cytometry analysis. *B*, BMDCs from either WT or TLR2-deficient mice (*TLR2 KO*) were incubated either with 1 μM Pam~$OVA_{247–264A5K}$ or *E. coli* LPS (10 μg/ml) for 48 h, and cells were treated as stated under *A*.

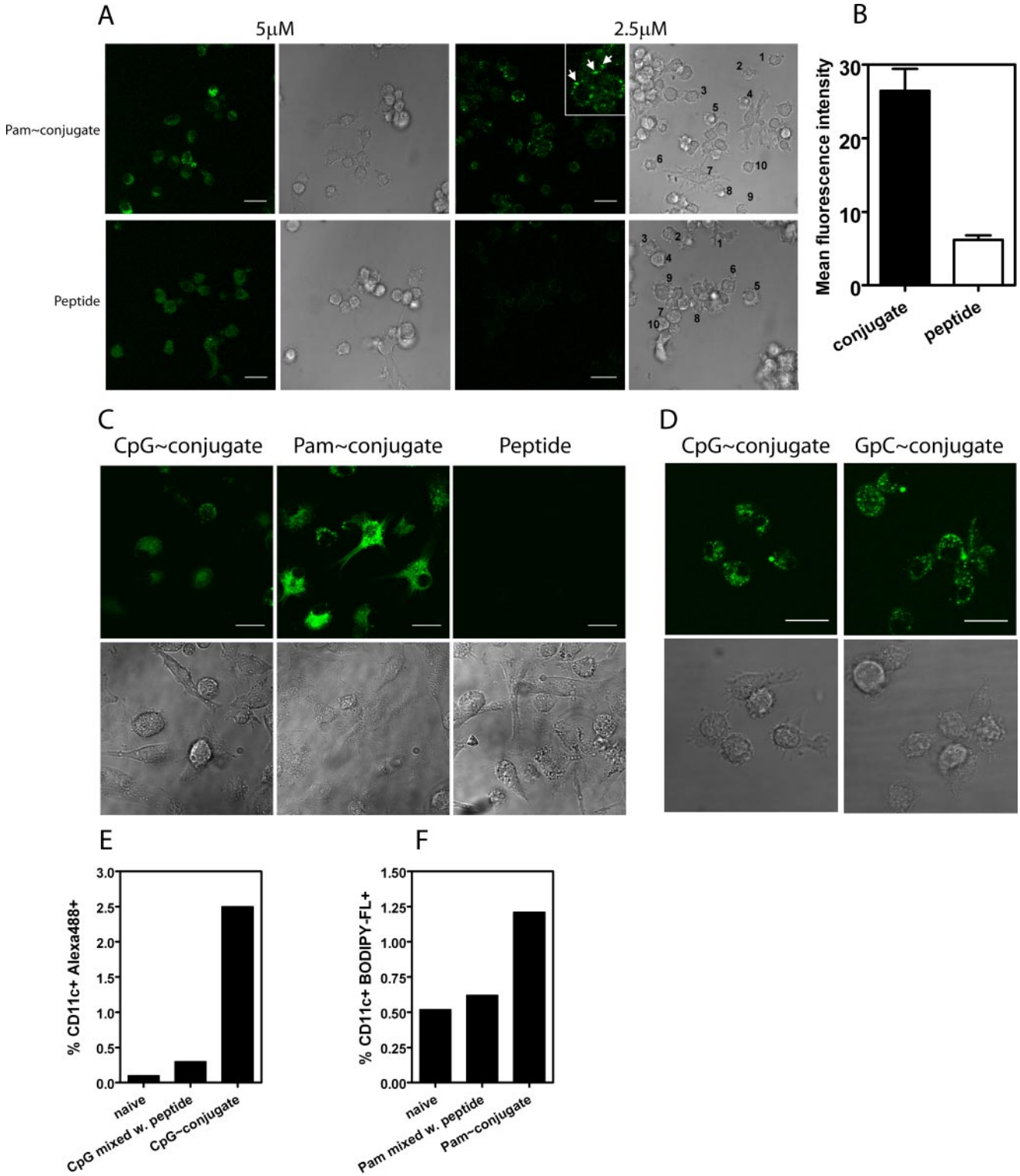

FIGURE 3. **Efficient antigen uptake mediated by the TLR-L conjugates.** *A*, confocal images of the dendritic cell line D1 incubated for 15 min with either BODIPY-FL labeled Pam~$OVA_{247-264}$ (*Pam~conjugate*) or BODIPY-FL-labeled peptide $OVA_{247-264}$ (*Peptide*) at different concentrations. *Arrows* indicate accumulation of Pam~conjugates. *B*, quantification of MFI of fluorescence inside numbered cells selected from *A*. *C*, DCs were incubated with either Alexa488 Fluor-labeled CpG~$OVA_{247-264}$ (*CpG~conjugate*), Pam~$OVA_{247-264}$ (*Pam~conjugate*), or $OVA_{247-264}$ peptide for 30 min; all compounds were used at 2.5 μM. *D*, DCs were incubated with either Alexa488 Fluor-labeled CpG~$OVA_{247-264}$ (*CpG~conjugate*) or GpC~$OVA_{247-264}$ (*GpC~conjugate*) for 30 min at a final concentration of 5 μM. All *scale bars* in *A–D* are 20 μm. *E*, mice were injected s.c. with either Alexa488 Fluor-labeled peptide $OVA_{247-264}$ mixed with CpG or Alexa488 Fluor-labeled CpG~$OVA_{247-264}$. 72 h later mice were sacrificed and drained lymph node cells were stained for CD11c. The *y* axis displays the percentages of Alexa488-positive cells out of total $CD11c^+$ cells. *F*, mice were injected s.c. with either BODIPY-FL-labeled peptide $OVA_{247-264}$ mixed with Pam or BODIPY-FL labeled Pam~$OVA_{247-264}$. 72 h later mice were sacrifices, and drained lymph node cells were stained for CD11c. The *y* axis displays the percentages of BODIPY-FL-positive cells out of total $CD11c^+$ cells. Experiments were conducted twice with similar results.

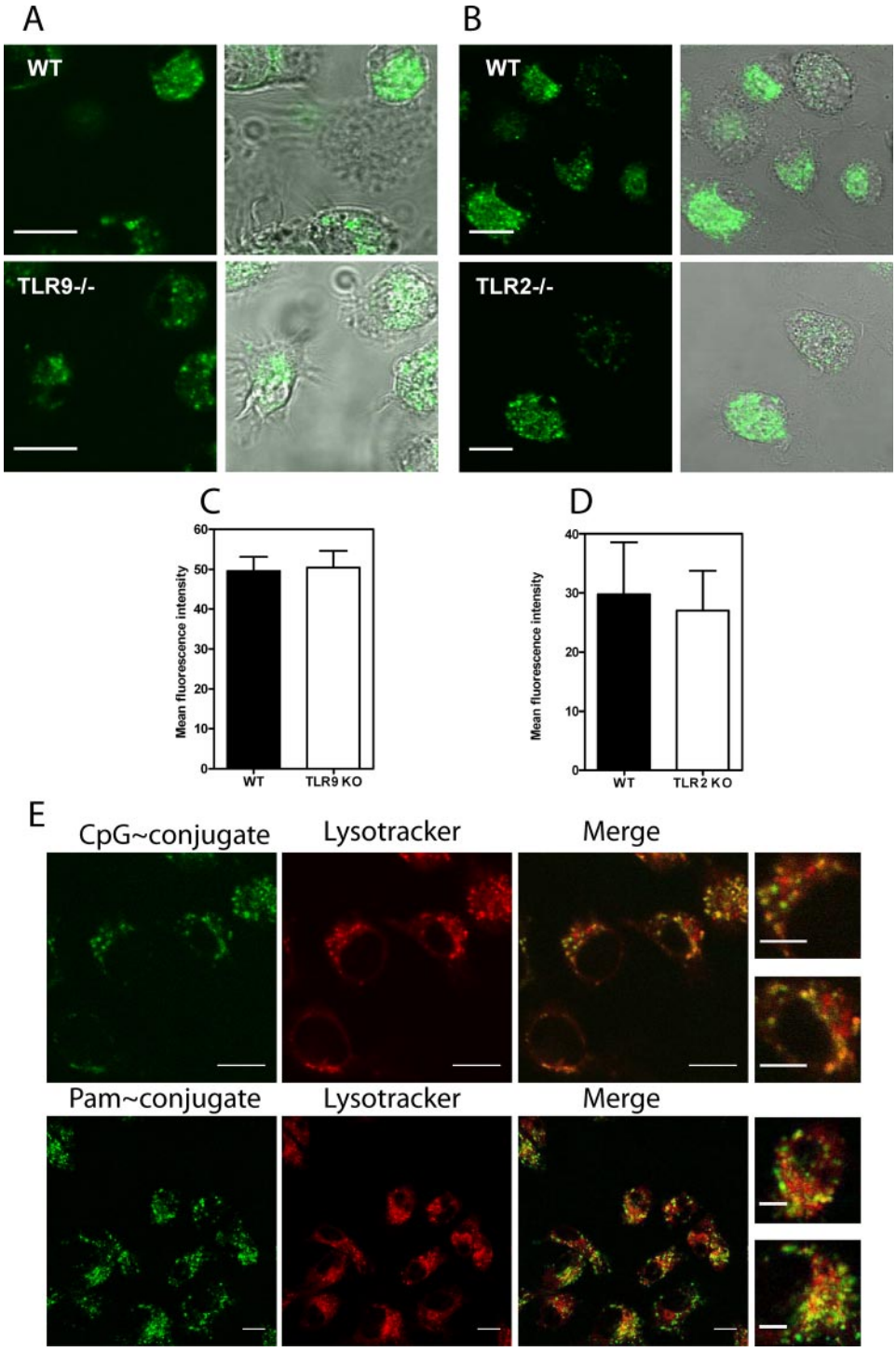

FIGURE 4. **TLR conjugates translocate to the endosomal compartment independently of TLR expression.** *A*, BMDCs from wild type mice or TLR9-deficient mice were incubated for 30 min with Alexa488 Fluor-labeled CpG~$OVA_{247–264}$ (5 μM). *B*, BMDCs from wild type mice or TLR2-deficient mice were incubated for 30 min with Alexa488 Fluor Pam~$OVA_{247–264}$ (2.5 μM). *Scale bars* in *A* and *B* are 15 μm. *C*, quantification of uptake of CpG~conjugate in BMDCs from WT and TLR9-deficient mice (*TLR9 KO*) was done on 10 random cells selected from similar pictures as depicted in *A*. *D*, quantification of uptake of the Pam~conjugate in BMDCs from WT and TLR2-deficient mice (*TLR2 KO*) was performed on 10 random cells selected from similar pictures as depicted in *B*. *E*, BMDCs were incubate with Alexa488 Fluor-labeled CpG~$OVA_{247–264}$ (5 μM) or Pam~$OVA_{247–264}$ (2.5 μM) in combination with 1 μM Lysotracker-DND99 before imaging. Images were acquired by sequential scanning, with only one laser line per scan to avoid cross-excitation. *Scale bars* are 10 μm and 5 μm in the enlarged images in the *right panel*.

or Pam mixed with the peptide, or the peptide alone (Fig. 5, *A* and *B*) before incubation with the peptide-specific T-cell hybridoma B3Z cells that recognize the H-$2K^b$, SIINFEKL CTL epitope (27). As the concentration of the compounds decreased, antigen recognition was rapidly lost when DCs were incubated either with the peptide alone or with the peptide mixed with CpG but not when the CpG~conjugated peptide was used. This indicates that the conjugation of peptides to TLR-L enhances antigen presentation (Fig. 5*A*). Likewise, an increased antigen presentation was observed for the Pam~conjugated peptide (Fig. 5*B*). In this case the difference in antigen presentation between conjugate and non-conjugate was even more prominent. Incubation with a mixture of free TLR-L (Pam or CpG) and the peptides resulted in a decreased antigen presentation by DCs when compared with loading with peptide alone or with conjugated peptide. This might be related to decreased uptake, since it has previously been reported that the endocytotic capacity of DCs declines upon encountering maturation signals (28, 29).

To gain insight in the kinetics of antigen presentation, DCs were incubated for various time periods with either TLR-L-conjugated peptide, peptide mixed with TLR-L, or peptide alone. As shown in Fig. 5, *C* and *D*, it required 24–48 h of continuous presence of peptide mixed with CpG or Pam or of peptide alone to reach the level of antigen presentation acquired already after 2 h of incubation with the conjugated peptide, as measured by an equal ability to stimulate the peptide-specific B3Z hybridoma T-cells. Thus, conjugation greatly improves the swiftness of presentation of antigen by DCs for stimulation of T-cells.

The confocal microscopy results indicated that uptake of the conjugates occurred independently from the expression of the respective TLRs. Therefore, we next evaluated the impact of TLR expression upon antigen presentation. To this end BMDCs from WT, $TLR2^{-/-}$, and $TLR9^{-/-}$ mice loaded with the conjugates were incubated *in vitro* together and subsequently incubated with the peptide-specific T-cell hybridoma

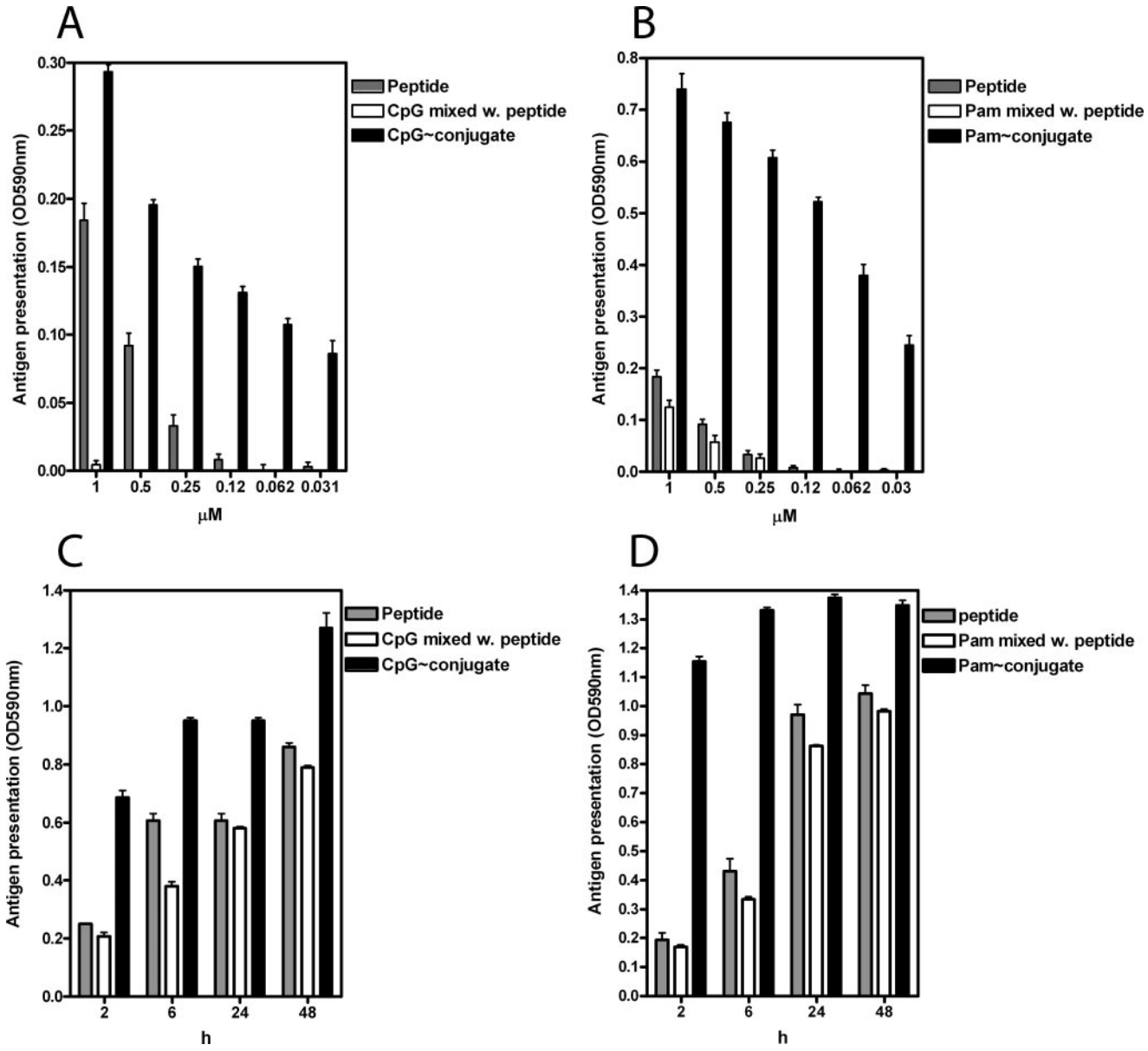

FIGURE 5. **TLR-L conjugates strongly enhance antigen presentation.** *A*, the dendritic cell line, D1, was incubated with either the $OVA_{247–264}$ peptide (*gray bars*), the $OVA_{247–264}$ peptide mixed with CpG (*white bars*), or CpG~conjugated to $OVA_{247–264}$ (*black bars*). After 2 h cells were washed, and B3Z cells were added and co-cultured for 24 h before their activation was measured. *B*, D1 cells were incubated under the same conditions as indicated under *A* but in the presence of either the $OVA_{247–264}$ peptide (*gray bars*), $OVA_{247–264}$ peptide mixed with Pam (*white bars*), or Pam-conjugated $OVA_{247–264}$ peptide (*black bars*). Results are the means of triplicates ± S.E. BMDCs were incubated for various time periods with either $OVA_{247–264A5K}$ (*gray bars*) CpG mixed with $OVA_{247–264A5K}$ peptide (*white bars*) or CpG~$OVA_{247–264A5K}$ (*black bars*) (*C*) or with $OVA_{247–264A5K}$ peptide (*gray bars*), Pam mixed with $OVA_{247–264A5K}$ (*white bars*), or Pam~$OVA_{247–264A5K}$ (*black bars*) (*D*) before co-culturing with B3Z T-cell hybridoma as outlined under "Experimental Procedures."

B3Z cell line. In line with the confocal uptake studies, BMDCs derived from WT or the TLR2- or TLR9-deficient mice strains were recognized to the same extent (Fig. 6, *A* and *B*).

Disruption of Clathrin Formation and Caveolae Clustering Blocks Antigen Presentation of TLR-L Conjugates—DCs can take up exogenous antigens via different mechanisms such as clathrin-mediated endocytosis, fluid phase endocytosis, and macropinocytosis (30). To define the pathways by which the TLR-L-peptide conjugates were internalized, DCs were pretreated with different inhibitors before loading with the TLR-L conjugates. Macropinocytosis inhibitor 5-(*N*,*N*-dimethyl)-amiloride (29) had no effect on antigen presentation.[5] On the other hand pretreatment with filipin, a sterol binding agent that disrupt caveolae structures (31) and thereby lipid-raft formation, reduced antigen presentation of both Pam~conjugates as well as CpG~conjugates in a dose-dependent manner, whereas antigen presentation of the CTL epitope $OVA_{257–264}$ was only marginal affected (Fig. 6*C*). Because lipid raft formation is involved both in clathrin-dependent endocytosis as well as caveolae-dependent internalization (32), we analyzed the impact of MDC, a specific inhibitor of clathrin formation (33, 34), upon antigen presentation. Interestingly, whereas antigen presentation of CpG~conjugated peptides was not affected by MDC, antigen presentation of Pam~conjugated peptides was abrogated in a dose-dependent fashion (Fig. 6*D*). To further explore the distinct uptake mechanisms used by the two types

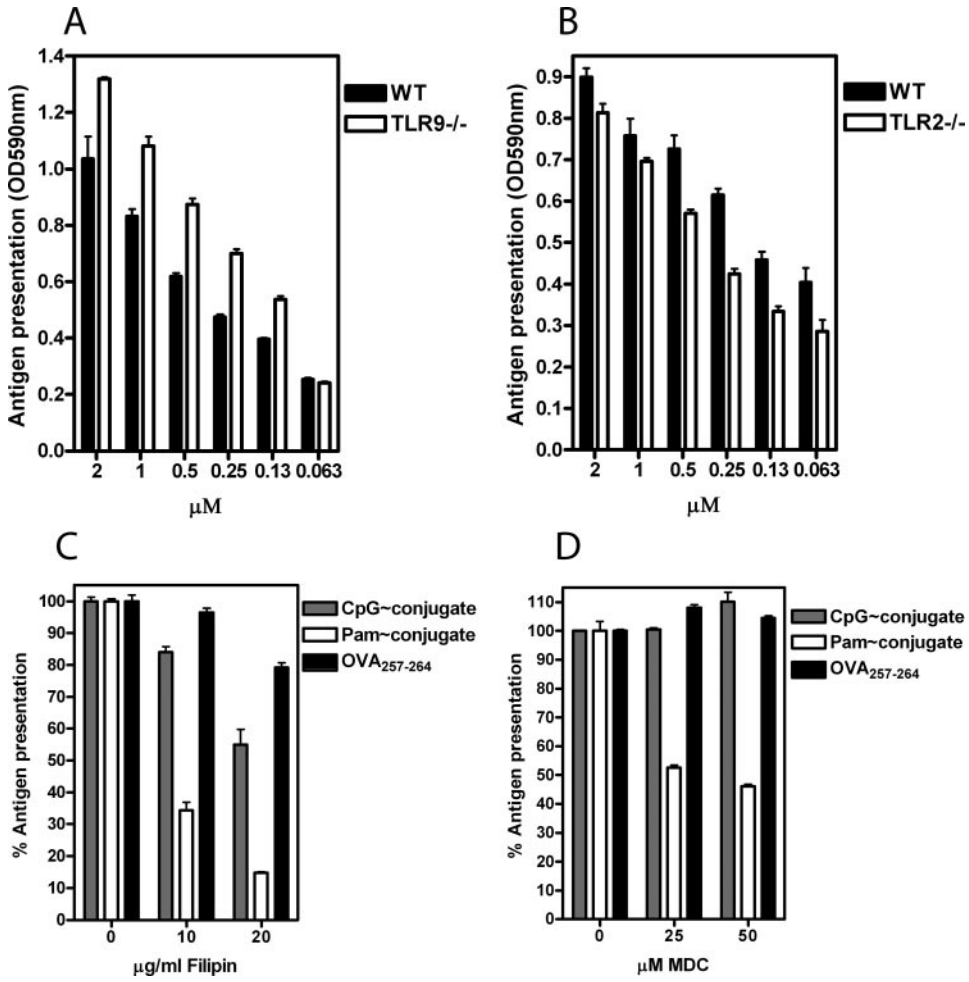

FIGURE 6. **Antigen presentation of TLR-L conjugates does not require TLR expression but is dependent on receptor-mediated endocytosis.** *A*, BMDCs from wild type mice (*black bars*) or TLR9 deficient mice (*white bars*) were incubated for 2 h with CpG~$OVA_{247–264}$ and processed for antigen presentation as described under "Experimental Procedures." *B*, BMDCs from wild type mice (*black bars*) or TLR2-deficient mice (*white bars*) were incubated for 2 h with Pam~$OVA_{247–264}$ and processed for antigen presentation. *C*, DCs were left untreated or were pretreated for 60 min with various concentrations of filipin or with various concentrations of MDC (*D*) before the addition of 0.5 μM CpG~$OVA_{247–264A5K}$ (*gray bars*), 0.5 μM Pam~$OVA_{247–264A5K}$ (*white bars*), or 0.01 μM $OVA_{257–264}$ (*black bars*). Cells were incubated with the peptides for 3 h in the presence of inhibitors before being processed as outlined under "Experimental Procedures." Actual optical density values in *C* in the absence of filipin were: CpG~conjugate, 0.5; Pam~conjugate, 1.4; $OVA_{257–264}$, 2.0. Actual optical density values in *D* in the absence of MDC were: CpG~conjugate, 0.5; Pam~conjugate, 1.0; $OVA_{257–264}$, 1.4. Background optical density levels of cells incubated without peptides were below 0.1 in both experiments.

of conjugates, confocal microscopy was performed on DCs treated with the two inhibitors. As evident from Fig. 7, both MDC and filipin abolished the internalization of the Pam conjugate in terms of mean fluorescence per cell, whereas inhibition of clathrin formation had a less pronounced effect on internalization of the CpG~conjugate (Fig. 7*C*). On the other hand, inhibition of caveolin formation by filipin reduced the mean fluorescence of cells incubated with the CpG~conjugate. The selective effect of the inhibitors was not due to a direct effect on one conjugate, as preincubation of cells with the inhibitor followed by extensive washing before incubation with the conjugates (indicated as preincubation in Fig. 7) in the absence of inhibitors led to similar results. Thus, these results indicate that the two TLR-L conjugates are internalized by distinct uptake receptors.

Antigen Presentation Depends upon Endosomal Acidification, Proteasome Activity, and TAP Translocation—Next, we examined the impact of different proteases upon antigen presentation. To address this issue, we made use of the C-terminal extended peptides ($OVA_{247–264A5K}$), which require both N-and C-terminal processing to release the SIINFEKL CTL peptide epitope. DCs were pretreated either with epoxomicin, which inhibits the proteasome, or NH_4Cl, which increases the pH in the acidic endosome/lysosome environment and thereby inhibits the proteases that depend on acidification (35–38) before incubation with either of the conjugates. As evident from Fig. 8, *A* and *B*, when DCs were pretreated with the lysosomotropic agent, NH_4Cl, a decrease in antigen presentation was seen ranging from 45% inhibition for the Pam~conjugates to 70% for the CpG~conjugated peptide. Similarly, inhibition of the proteasome activity resulted in an overall decrease in antigen presentation of both the CpG~conjugated and Pam~conjugated peptide (up to 50% inhibition) in a dose-dependent manner (Fig. 8*C*). To ascertain that the inhibitory effect observed was not due to an overall decrease in the surface expression of MHC class I, DCs that had been pretreated with either epoxomicin or NH_4Cl were incubated with the minimal CTL epitope $OVA_{257–264}$. As expected, the inhibitors did not cause a major affect upon antigen presentation of exogenous loaded $OVA_{257–264}$ peptide (Fig. 8, *B* and *C*).

After proteasomal processing, CTL peptide epitopes need to be translocated into the luminal side of the endoplasmic reticulum via the transporter complex TAP to be loaded onto MHC class I molecules. To address the involvement of TAP for cross presentation of the TLR-L conjugates, BMDCs from either wild type mice or TAP-deficient mice were loaded with the TLR-L conjugates or the minimal CTL epitope $OVA_{257–264}$. As evident in Fig. 8*D*, antigen presentation of both the TLR2L and TLR9L conjugates depended upon TAP activity, as the presentation was abrogated in TAP-deficient mice. Importantly, antigen presentation of the minimal CTL epitope $OVA_{257–264}$ was not affected in the TAP-deficient DCs, showing that the observed TAP dependence of the conjugates was not due to an overall reduced surface expression of MHC class I in the TAP-deficient DCs. In contrast, when using BMDCs from mice deficient in both TAP and β2-microglobulin expression ($TAP^{-/-}$ $\beta 2m^{-/-}$) completely lacking MHC class I surface expression (39), antigen presentation was completely lost for all peptides (Fig. 8*D*).

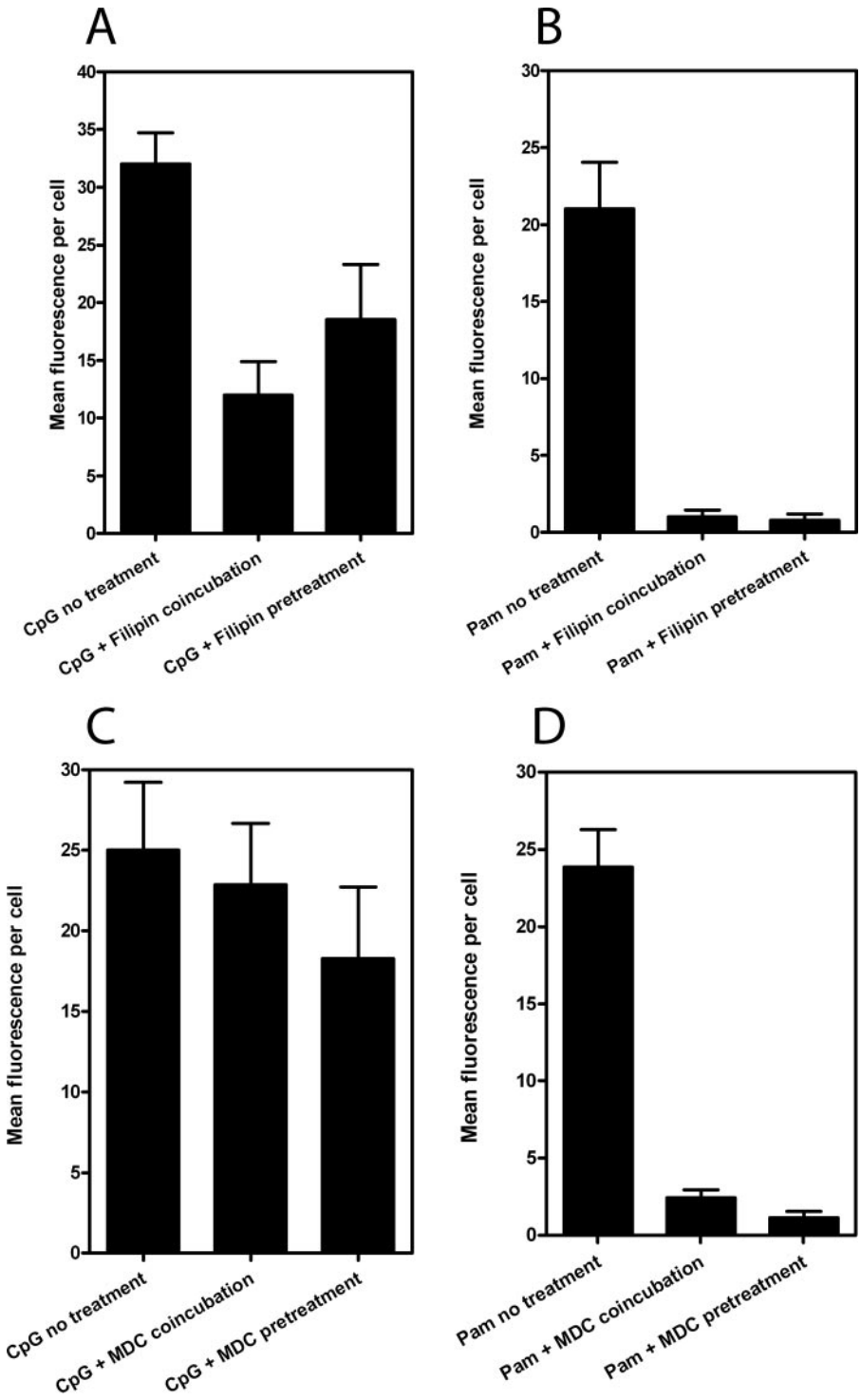

FIGURE 7. **Effect of filipin and MDC on internalization of the TLR-L conjugates.** DCs were left untreated or pretreated for 30 min with 10 μg/ml filipin before adding Alexa488-labeled CpG~conjugate (*A*) or BODIPY-FL labeled Pam~conjugate (*B*) either in the presence of filipin (*coincubation*) or in the absence of filipin (*pretreatment*) for 30 min at 37 °C before being subjected to confocal microscopy analysis. DCs were left untreated or pretreated for 30 min with 50 μM MDC before adding Alexa488-labeled CpG~conjugate (*C*) or BODIPY-FL labeled Pam~conjugate (*D*) either in the presence of MDC (*coincubation*) or in the absence of MDC (*pretreatment*) for 30 min at 37 °C before being subjected to confocal microscopy analysis. Shown is the mean fluorescence intensity per cell based on quantification of 10 random selected cells.

Collectively, these results indicate that endosomal acidification, proteasomal activity, and TAP translocation are required for antigen presentation of the TLR-L peptide conjugates and suggest that the peptide (conjugate) translocates via the endosomal compartment into the cytosol where the peptide undergoes proteasomal processing before being loaded onto MHC class I molecules in the endoplasmic reticulum.

DISCUSSION

In this study we analyzed the cellular uptake and trafficking of two distinct TLR ligand-antigen conjugates that ultimately lead to the induction of an efficient CTL response. Strikingly, one single s.c. immunization with conjugate in saline induced an impressive systemic expansion of antigen-specific CD8 T-cells (Fig. 1). Thus, conjugation resulted in a stronger systemic response than what was observed for the mixed vaccines.

Our immunofluorescence analysis revealed that conjugates of both types of TLR ligands were taken up very efficiently compared with unconjugated peptides (Fig. 3). Internalization was a very rapid process since uptake studies showed that already within 15–30 min, the major part of the conjugates could be found in endosome/lysosome compartments (Fig. 4).[5] For this we have used fluorescent conjugates; these may have slightly different properties from those of the unmodified conjugates, which could influence the uptake and function. However, the fluorescent conjugates induced DC maturation to a similar extent as the unmodified conjugates.[5] In line with our findings, CpG linked to fluorescein isothiocyanate-labeled ovalbumin protein was recently shown to translocate to LAMP-1-positive endosomal-lysosomal compartments (10). Further support of enhanced uptake mediated by the conjugates was provided from our *in vivo* uptake analysis, which revealed a 6–8-fold increase in uptake of the CpG-conjugated peptide by $CD11c^+$ cells and a 2-fold increase in uptake of the Pam-conjugated peptide by $CD11c^+$ cells compared with uptake of non-conjugated peptide (Fig. 3, *E* and *F*). We found that CpG~conjugated peptides were internalized independently from the expression

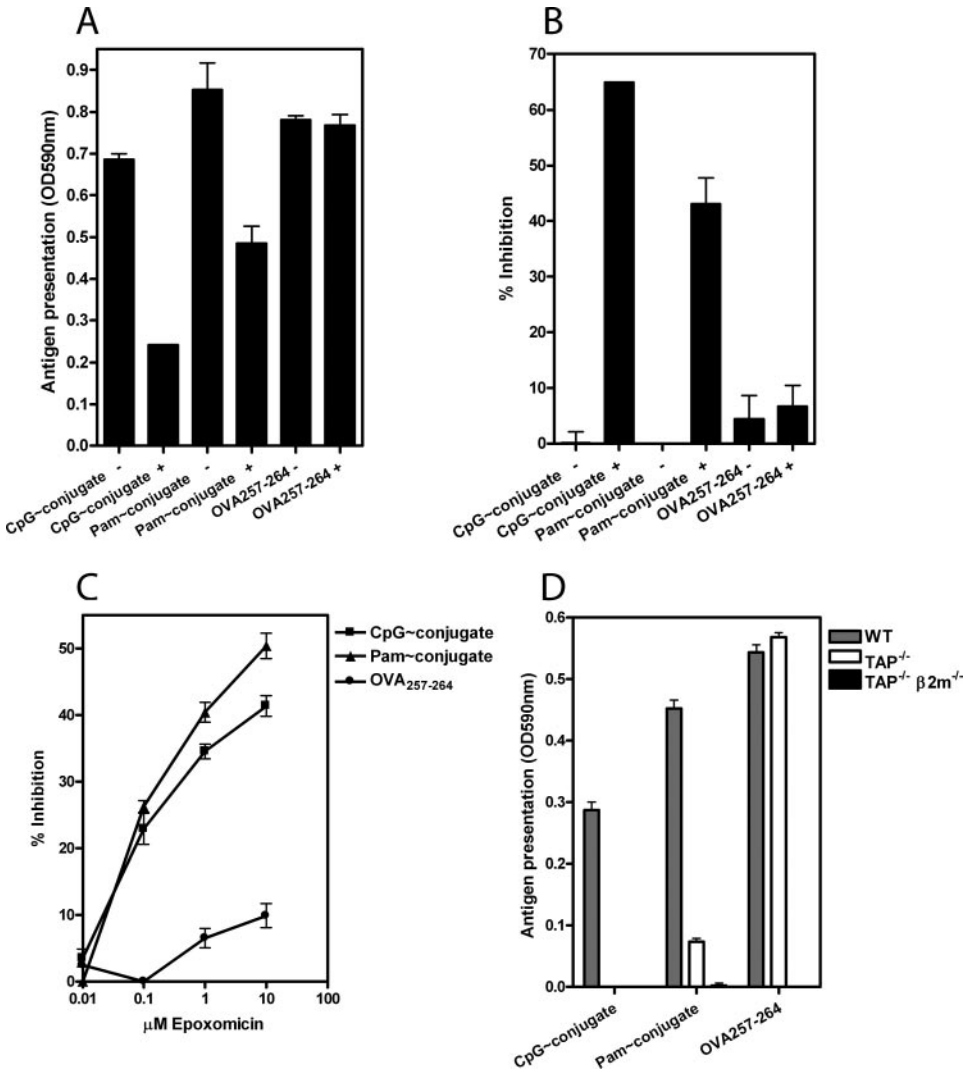

FIGURE 8. **Antigen presentation depends upon endosomal acidification, proteasomal activity, and TAP translocation.** DCs were left untreated or pretreated for 60 min with various concentrations of 3 mM NH_4Cl (*A*) and (*B*), or epoxomicin (*C*) before the addition of 0.5 μM CpG~$OVA_{247-264A5K}$ (*squares*), 0.5 μM Pam~$OVA_{247-264A5K}$ (*triangles*), or 0.01 μM $OVA_{257-264}$ (*circles*). Cells were incubated with the peptides for 3 h in the presence of inhibitors before being processed as outlined under "Experimental Procedures." −, untreated; +, treated with NH_4Cl. Results are the means of triplicates ±S.E. *D*, BMDCs from WT mice, TAP-deficient mice (*TAP*$^{-/-}$), or mice deficient in TAP and β2-microglobulin (*TAP*$^{-/-}$ *β2m*$^{-/-}$) were preloaded either with CpG-conjugates, Pam-conjugate, or $OVA_{257-264}$ before being processed as outlined under "Experimental Procedures."

of TLR9 and could also support antigen presentation *in vitro* independently of TLR9 expression (Fig. 4). Accordingly, Wagner and co-workers (2) showed that cross-presentation of OVA-linked CpG occurred independently from TLR9 expression but that TLR9 expression nevertheless was essential for activation of the DCs. At first sight these findings might seem paradoxical; however, TLR9 are mainly expressed in the endoplasmic reticulum followed by recruitment to the endosomes upon dendritic cell maturation (40).

Unexpectedly, considering the cell surface expression of TLR2, we found that internalization of the Pam~conjugate was taken up independently from the expression of TLR2. BMDCs isolated from TLR2-deficient mice internalized the Pam~conjugate to a comparable level as BMDCs from wild type mice, and antigen recognition was unaffected in BMDCs from TLR2-deficient mice. This could not be attributed to a side effect mediated by the peptide part, since TLR2-independent internalization was also observed when incubating the cells with free Pam.[5] Importantly, inhibition of clathrin-dependent endocytosis or caveolae formation abrogated both uptake and antigen presentation of Pam conjugates (Figs. 6 and 7), whereas internalization of CpG conjugates was independent of clathrin-coated pits but dependent on caveolae formation. These results indicate that other (distinct) receptors than the TLRs are involved in the uptake of the TLR conjugates, although the exact nature of these receptors remains to be established. Other TLR2 ligands have been reported to be internalized independently from the expression of TLR2. Outer membrane protein A, a conserved major component of the outer membrane of *Enterobacteriaceae* family that triggers cytokine production in macrophages and DCs (41), was recently shown to be internalized by the scavenger receptor LOX-1 independently from the expression of TLR2 (42). Moreover, lipoteichoic acid has also been reported to be internalized independently from TLR2 expression (43), although the receptor involved in the uptake of lipoteichoic acid still remains to be identified. Therefore, the contribution of TLR2 and other receptors expressed on the cell surface to the uptake of Pam and other TLR ligands remains to be established.

Optimal presentation of the peptide antigen cargo in the conjugates required endosomal acidification (Fig. 8), although it cannot be ruled out that the fusion of early endosomal vesicles with late endosomal vesicles is hampered by the lysosomotropic agent NH_4Cl (37, 44–46).These results imply that endosomal proteases, such as cathepins (45, 47), might be involved in the processing of the TLR-L-peptide conjugate. Furthermore, proteasomal cleavage was required because proteasome inhibition greatly decreased antigen presentation of the TLR-L conjugates (Fig. 8*C*). Because proteasomes are mainly located in the cytosol (48, 49), our results indicate that the peptide/conjugate, after being released in the endosomal compartment, translocate to the cytosol to undergo proteasomal processing (45). In this regard it was recently reported that the translocon complex SEC61 could be involved in facilitating the translocation of peptide from the endosomes to the cytosol (50). Moreover, abrogation of translocation of

peptides from the cytosol to the endoplasmic reticulum completely abrogated antigen presentation of both types of TLR-L-peptide conjugates (Fig. 8*D*). Aside from being internalized efficiently, we found that all of the TLR-L conjugates retained their capacity to activate DCs to a comparable level as the free TLR-L both in terms of production of the Th1-favoring cytokine, IL-12,[5] and up-regulation of DC maturation surface markers (Table 2). Importantly, TLR expression was required for DC activation, since BMDCs lacking TLR2 or TLR9 were not able to up-regulate co-stimulatory molecules upon stimulation with either Pam~conjugate or CpG~conjugate, respectively (Fig. 2). In addition, conjugation of the non-stimulatory GpC oligonucleotide to the peptide antigen resulted in inefficient CTL priming (Fig. 1), showing that the DC activation of TLR-L peptide conjugates is essential. Therefore, intracellular signaling of TLR is crucially important for effective CTL priming by the conjugates.

In summary, we demonstrate that well defined synthetic TLR-L-peptide conjugates induce a robust and systemic response of specific T-cells due to the combined action of enhanced antigen uptake, improved MHC class I antigen presentation, and dendritic cell maturation. Our data show that targeting to two different TLRs requires a distinct uptake mechanism independent of TLR expression but follows similar trafficking and intracellular processing pathways leading to optimal antigen presentation and T-cell priming. The chemical properties of these conjugates, which ensure that the same DCs that take up the antigen receives simultaneously a proper maturation signal, is likely to be the mechanism behind the superior activity of the peptide conjugates. Accordingly, Medzhitov and Blander (51) recently reported that synchronous entrance of TLR-L and antigen enhanced MHC class II presentation, although in their system antigen and TLR-L was delivered on microspheres in a non-covalent manner. The collective features of our TLR-L peptide conjugates together with their convenient manufacture and handling makes synthetic peptide-TLR-ligand conjugates an attractive novel vaccine modality.

Acknowledgments—We thank Dr. M. Haks for critical reading the manuscript and Dr. R. Sutmuller for assistance with generation of TLR9$^{-/-}$ bone marrow-derived dendritic cells.

REFERENCES

1. Kaisho, T., and Akira, S. (2004) *Microbes Infect.* **6,** 1388–1394
2. Heit, A., Maurer, T., Hochrein, H., Bauer, S., Huster, K. M., Busch, D. H., and Wagner, H. (2003) *J. Immunol.* **170,** 2802–2805
3. Miggin, S. M., and O'Neill, L. A. (2006) *J. Leukocyte Biol.* **80,** 220–226
4. Riezman, H., Woodman, P. G., van Meer, G., and Marsh, M. (1997) *Cell* **91,** 731–738
5. Guermonprez, P., Valladeau, J., Zitvogel, L., Thery, C., and Amigorena, S. (2002) *Annu. Rev. Immunol.* **20,** 621–667
6. Xiang, S. D., Scholzen, A., Minigo, G., David, C., Apostolopoulos, V., Mottram, P. L., and Plebanski, M. (2006) *Methods* **40,** 1–9
7. Yewdell, J. W., Reits, E., and Neefjes, J. (2003) *Nat. Rev. Immunol.* **3,** 952–961
8. Schuurhuis, D. H., Laban, S., Toes, R. E., Ricciardi-Castagnoli, P., Kleijmeer, M. J., van der Voort, E. I., Rea, D., Offringa, R., Geuze, H. J., Melief, C. J., and Ossendorp, F. (2000) *J. Exp. Med.* **192,** 145–150
9. Heath, W. R., Belz, G. T., Behrens, G. M., Smith, C. M., Forehan, S. P., Parish, I. A., Davey, G. M., Wilson, N. S., Carbone, F. R., and Villadangos, J. A. (2004) *Immunol. Rev.* **199,** 9–26
10. Heit, A., Schmitz, F., O'Keeffe, M., Staib, C., Busch, D. H., Wagner, H., and Huster, K. M. (2005) *J. Immunol.* **174,** 4373–4380
11. Horner, A. A., Datta, S. K., Takabayashi, K., Belyakov, I. M., Hayashi, T., Cinman, N., Nguyen, M. D., Van Uden, J. H., Berzofsky, J. A., Richman, D. D., and Raz, E. (2001) *J. Immunol.* **167,** 1584–1591
12. Shirota, H., Sano, K., Hirasawa, N., Terui, T., Ohuchi, K., Hattori, T., Shirato, K., and Tamura, G. (2001) *J. Immunol.* **167,** 66–74
13. Tighe, H., Takabayashi, K., Schwartz, D., Van Nest, G., Tuck, S., Eiden, J. J., Kagey-Sobotka, A., Creticos, P. S., Lichtenstein, L. M., Spiegelberg, H. L., and Raz, E. (2000) *J. Allergy Clin. Immunol.* **106,** 124–134
14. Zeng, W., Ghosh, S., Lau, Y. F., Brown, L. E., and Jackson, D. C. (2002) *J. Immunol.* **169,** 4905–4912
15. Cho, H. J., Takabayashi, K., Cheng, P. M., Nguyen, M. D., Corr, M., Tuck, S., and Raz, E. (2000) *Nat. Biotechnol.* **18,** 509–514
16. Maurer, T., Heit, A., Hochrein, H., Ampenberger, F., O'Keeffe, M., Bauer, S., Lipford, G. B., Vabulas, R. M., and Wagner, H. (2002) *Eur. J. Immunol.* **32,** 2356–2364
17. Matyszak, M. K., Citterio, S., Rescigno, M., and Ricciardi-Castagnoli, P. (2000) *Eur. J. Immunol.* **30,** 1233–1242
18. Winzler, C., Rovere, P., Rescigno, M., Granucci, F., Penna, G., Adorini, L., Zimmermann, V. S., Davoust, J., and Ricciardi-Castagnoli, P. (1997) *J. Exp. Med.* **185,** 317–328
19. Sanderson, S., and Shastri, N. (1994) *Int. Immunol.* **6,** 369–376
20. Moore, M. W., Carbone, F. R., and Bevan, M. J. (1988) *Cell* **54,** 777–785
21. Chan, W. C., and White, P. D. (2000) in *Fmoc Solid Phase Peptide Synthesis: A Practical Approach* (Chan, W. C., and White, P. D., eds) pp. 41–74, Oxford University Press, New York
22. Grandas, A., Marchan, V., Debethune, L., and Pedroso, E. (2003) in *Current Protocols in Nucleic Acid Chemistry* (Beaucage, S. L., Bergstrom, D. E., Glick, G. D., Jones, R. A., eds) pp. 4.22.1–4.22.54, John Wiley & Sons, Inc., New York
23. Schuurhuis, D. H., Ioan-Facsinay, A., Nagelkerken, B., van Schip, J. J., Sedlik, C., Melief, C. J., Verbeek, J. S., and Ossendorp, F. (2002) *J. Immunol.* **168,** 2240–2246
24. Stukart, M. J., Boes, J., and Melief, C. J. (1984) *J. Immunol.* **133,** 24–27
25. Banchereau, J., Briere, F., Caux, C., Davoust, J., Lebecque, S., Liu, Y. J., Pulendran, B., and Palucka, K. (2000) *Annu. Rev. Immunol.* **18,** 767–811
26. Kaisho, T., and Akira, S. (2001) *Acta Odontol. Scand.* **59,** 124–130
27. Karttunen, J., and Shastri, N. (1991) *Proc. Natl. Acad. Sci. U. S. A.* **88,** 3972–3976
28. Mellman, I., and Steinman, R. M. (2001) *Cell* **106,** 255–258
29. Sallusto, F., Cella, M., Danieli, C., and Lanzavecchia, A. (1995) *J. Exp. Med.* **182,** 389–400
30. Steinman, R. M., Inaba, K., Turley, S., Pierre, P., and Mellman, I. (1999) *Hum. Immunol.* **60,** 562–567
31. Rothberg, K. G., Heuser, J. E., Donzell, W. C., Ying, Y. S., Glenney, J. R., and Anderson, R. G. (1992) *Cell* **68,** 673–682
32. Nichols, B. J., Kenworthy, A. K., Polishchuk, R. S., Lodge, R., Roberts, T. H., Hirschberg, K., Phair, R. D., and Lippincott-Schwartz, J. (2001) *J. Cell Biol.* **153,** 529–541
33. Bradley, J. R., Johnson, D. R., and Pober, J. S. (1993) *J. Immunol.* **150,** 5544–5555
34. Nandi, P. K., Van Jaarsveld, P. P., Lippoldt, R. E., and Edelhoch, H. (1981) *Biochemistry* **20,** 6706–6710
35. Sin, N., Kim, K. B., Elofsson, M., Meng, L., Auth, H., Kwok, B. H., and Crews, C. M. (1999) *Bioorg. Med. Chem. Lett.* **9,** 2283–2288
36. Schwarz, K., de Giuli, R., Schmidtke, G., Kostka, S., van den, B. M., Kim, K. B., Crews, C. M., Kraft, R., and Groettrup, M. (2000) *J. Immunol.* **164,** 6147–6157
37. Mellman, I., Fuchs, R., and Helenius, A. (1986) *Annu. Rev. Biochem.* **55,** 663–700
38. Kalina, M., and Socher, R. (1991) *J. Histochem. Cytochem.* **39,** 1337–1348
39. Ljunggren, H. G., Van Kaer, L., Sabatine, M. S., Auchincloss, H., Jr., Tonegawa, S., and Ploegh, H. L. (1995) *Int. Immunol.* **7,** 975–984
40. Latz, E., Schoenemeyer, A., Visintin, A., Fitzgerald, K. A., Monks, B. G., Knetter, C. F., Lien, E., Nilsen, N. J., Espevik, T., and Golenbock, D. T. (2004) *Nat. Immunol.* **5,** 190–198

41. Jeannin, P., Magistrelli, G., Goetsch, L., Haeuw, J. F., Thieblemont, N., Bonnefoy, J. Y., and Delneste, Y. (2002) *Vaccine* **20,** Suppl. 4, 23–27
42. Jeannin, P., Bottazzi, B., Sironi, M., Doni, A., Rusnati, M., Presta, M., Maina, V., Magistrelli, G., Haeuw, J. F., Hoeffel, G., Thieblemont, N., Corvaia, N., Garlanda, C., Delneste, Y., and Mantovani, A. (2005) *Immunity* **22,** 551–560
43. Triantafilou, M., Manukyan, M., Mackie, A., Morath, S., Hartung, T., Heine, H., and Triantafilou, K. (2004) *J. Biol. Chem.* **279,** 40882–40889
44. Seglen, P. O. (1983) *Methods Enzymol.* **96,** 737–764
45. Yewdell, J. W., Norbury, C. C., and Bennink, J. R. (1999) *Adv. Immunol.* **73,** 1–77
46. Hart, P. D., and Young, M. R. (1991) *J. Exp. Med.* **174,** 881–889
47. Shen, L., Sigal, L. J., Boes, M., and Rock, K. L. (2004) *Immunity* **21,** 155–165
48. Tanaka, K., Ii, K., Ichihara, A., Waxman, L., and Goldberg, A. L. (1986) *J. Biol. Chem.* **261,** 15197–15203
49. Tanaka, K., Kumatori, A., Ii, K., and Ichihara, A. (1989) *J. Cell. Physiol.* **139,** 34–41
50. Ackerman, A. L., Giodini, A., and Cresswell, P. (2006) *Immunity.* **25,** 607–617
51. Blander, J. M., and Medzhitov, R. (2006) *Nature* **440,** 808–812

Distinct Uptake Mechanisms but Similar Intracellular Processing of Two Different Toll-like Receptor Ligand-Peptide Conjugates in Dendritic Cells

Selina Khan, Martijn S. Bijker, Jimmy J. Weterings, Hans J. Tanke, Gosse J. Adema, Thorbald van Hall, Jan W. Drijfhout, Cornelis J. M. Melief, Hermen S. Overkleeft, Gijsbert A. van der Marel, Dmitri V. Filippov, Sjoerd H. van der Burg and Ferry Ossendorp

J. Biol. Chem. 2007, 282:21145-21159.
doi: 10.1074/jbc.M701705200 originally published online April 26, 2007
